

## Two-scale scalar mesons in nuclei

K. Saito<sup>1,a</sup>, H. Kouno<sup>2</sup>, K. Tsushima<sup>3</sup>, and A.W. Thomas<sup>4</sup>

<sup>1</sup> Department of Physics, Faculty of Science and Technology, Tokyo University of Science, Noda 278-8510, Japan

<sup>2</sup> Department of Physics, Saga University, Saga 840-8502, Japan

<sup>3</sup> Physics Division, National Center for Theoretical Sciences, Taipei 10617, Taiwan

<sup>4</sup> Thomas Jefferson National Accelerator Facility, 12000 Jefferson Ave., Newport News, VA 23606, USA

Received: 22 August 2005 / Revised version: 17 November 2005 /

Published online: 1 December 2005 – © Società Italiana di Fisica / Springer-Verlag 2005

Communicated by V. Vento

**Abstract.** We generalize the linear  $\sigma$  model in order to develop a chiral-invariant model of the nuclear structure. The model is *natural*, and contains not only the usual  $\sigma$ -meson which is the chiral partner of the pion but also a new chiral singlet that is responsible for the medium-range nucleon-nucleon attraction. This approach provides significant advantages in terms of its description of nuclear matter and finite nuclei in comparison with conventional models based on the linear  $\sigma$  model.

**PACS.** 11.30.Rd Chiral symmetries – 21.65.+f Nuclear matter

### 1 Introduction

Phenomenological relativistic field theories can provide a satisfactory description of the properties of nuclear matter and finite nuclei [1, 2]. The fundamental importance of chiral symmetry means that it must be incorporated into models of this kind. As a result, there is a long history of attempts to generalize the linear  $\sigma$  model ( $L\sigma M$ ) to build nuclear models with chiral symmetry (the pioneering work can be seen in ref. [3]). However, it is well known that the  $L\sigma M$ , supplemented by a repulsive force associated with  $\omega$  exchange, leads to bifurcations in the equation of state (EOS) [4, 5] and that the model usually gives a very large incompressibility,  $K$ , and, hence, a very stiff EOS. The bifurcation problem may be settled 1) by introducing a  $\sigma$ - $\omega$  coupling in the mean-field approximation (MFA) [5, 6] and 2) in the one-loop approximation due to a modified effective potential [7]. Further studies on the chiral nuclear model can be found in refs. [8, 9].

It is, however, difficult to build relativistic mean-field phenomenology with manifest chiral symmetry based upon the conventional  $L\sigma M$ , which contains a scalar meson, *i.e.* the  $\sigma$ -meson, playing a dual role as the chiral partner of the pion *and* the mediator of the medium-range nucleon-nucleon (NN) attraction [10]. Chiral perturbation theory actually forbids the identification of this NN attraction with the exchange of the  $\sigma$ . In the  $L\sigma M$ , two critical constraints are imposed: one is the “Mexican hat” potential, which gives a very strong nonlinearity of the scalar field, and the other is the equality between the scalar and

pion couplings to the nucleon. The latter eventually requires a large value ( $\geq 600$  MeV) of the  $\sigma$  mass and leads to unrealistic, oscillating nuclear charge densities, level ordering and shell closures [10]. Furthermore, as is well known, the predictions of the  $L\sigma M$  generally involve cancellations among several graphs. One example is the  $\pi N$  scattering amplitude where the  $\sigma$  exchange combining with the Born term satisfies the soft-pion results, whose magnitude is too small.

An alternative is to adopt a nonlinear realization of chiral symmetry. To avoid the unnatural cancellations of the  $L\sigma M$ , the  $\sigma$  field is eliminated by imposing the constraint that the fields lie on the chiral circle,  $\sigma^2 + \pi^2 = f_\pi^2$  (with  $f_\pi$  the pion decay constant), in the nonlinear model (NLM). This is all fine for chiral symmetry. However, at mean-field level, it is somewhat frustrating for nuclear physics because it is not easy to introduce a scalar-isoscalar channel which is responsible for the mid-range NN attraction. When studying only elementary processes, it is a matter of taking care of the cancellations but when studying the nuclear many-body problem in MFA, it is certainly much simpler to introduce a scalar-isoscalar meson explicitly.

In the usual NLM, the chiral radius is fixed to  $f_\pi$  by mere convenience. However, nothing prevents us from keeping the fluctuation of the chiral circle as a degree of freedom, and identifying it with the meson which yields the mid-range attraction. Chanfray *et al.* [11] have proposed a chiral nuclear model in which the  $L\sigma M$  is reformulated in the standard nonlinear form as far as the pion field is concerned but where the scalar degree of freedom

<sup>a</sup> e-mail: ksaito@ph.noda-tus.ac.jp

(called  $\theta$ ), corresponding to fluctuations along the chiral radius, is maintained. Thus, the model explicitly involves the scalar meson for the NN attraction but does not have the unnatural cancellations. However, in their calculation the mass of the  $\theta$ -meson was predicted to be in the range 0.8–1.0 GeV, which may again be too large to obtain good fits to the properties of finite nuclei.

Combining nonlinear chiral symmetry with the broken scale invariance of QCD is another approach to construct a nuclear model [12]. In such a model, the low-energy theorems involving the QCD trace anomaly of the energy-momentum tensor are *assumed* to be saturated by a scalar glueball (gluonium) field with a large (above 1 GeV) mass *and* a light scalar field. Thus, two different scales are required in the scalar channel. After integrating out the heavy gluonium field, one can construct an effective model which contains the chiral-singlet scalar field with a mass of about 400–500 MeV. Since the light scalar meson can be responsible for the mid-range NN attraction, the model provides good fits to the bulk properties of finite nuclei and single-particle spectra. However, this does not involve the scalar field which corresponds to the fluctuation of the chiral radius.

Even in the L $\sigma$ M, if a new, light scalar field which phenomenologically simulates the mid-range attractive NN force is introduced not as the chiral partner of the pion but as a chiral singlet, one may be able to construct a new chiral-invariant model. In this article, we construct such a model and study the role of scalar mesons in symmetric nuclear matter as well as finite nuclei (see also ref. [13]). As discussed above, it may be necessary to include at least two kinds of scalar mesons: the usual  $\sigma$ -meson with a relatively large mass and a new, chiral-singlet scalar meson with a light mass. The  $\sigma$ -meson is the chiral partner of the pion and they form an isoscalar-isovector scalar quartet,  $(\sigma, \boldsymbol{\pi})$ . The fluctuations around the stable point on the chiral circle are described by them. When the  $\sigma$  mass is large, the  $\sigma$  field itself is relatively reduced in matter and it is hence expected that the “Mexican hat” potential producing the undesirable, strong nonlinearity of the  $\sigma$  field would also be suppressed. In contrast, because of its small mass, the new scalar field is enhanced and it may provide the main part of the NN attraction. Our underlying philosophy is that the NN attraction in matter is simply dominated by scalar-isoscalar, correlated two-pion exchange and that it is this that is being simulated by the light scalar meson in MFA.

## 2 Lagrangian

Let us first start from the Lagrangian density of the L $\sigma$ M with an explicit symmetry breaking term,

$$\mathcal{L} = \mathcal{L}_0 + \mathcal{L}_{SB}, \quad (1)$$

where

$$\begin{aligned} \mathcal{L}_0 = & \bar{\psi}[i\gamma^\mu\partial_\mu - g_0(\sigma + i\boldsymbol{\tau} \cdot \boldsymbol{\pi}\boldsymbol{\gamma}_5)]\psi \\ & + \frac{1}{2}(\partial_\mu\sigma\partial^\mu\sigma + \partial_\mu\boldsymbol{\pi} \cdot \partial^\mu\boldsymbol{\pi}) - \frac{\lambda}{4}(\sigma^2 + \boldsymbol{\pi}^2 - v^2)^2, \quad (2) \end{aligned}$$

and  $\mathcal{L}_{SB} = c\sigma$  with  $\sigma$  and  $\boldsymbol{\pi}$  the  $\sigma$  and  $\pi$  fields, respectively. Next we introduce a chiral-invariant Lagrangian density for the chiral-singlet scalar meson  $s$ :

$$\mathcal{L}_s = \frac{g_s}{f_\pi}\bar{\psi}(\sigma + i\boldsymbol{\tau} \cdot \boldsymbol{\pi}\boldsymbol{\gamma}_5)F(s)\psi + \frac{1}{2}(\partial_\mu s\partial^\mu s - m_s^2 s^2), \quad (3)$$

with  $g_s$  the strength of the  $s$ -N coupling and  $m_s$  the  $s$ -meson mass. The first term describes the interaction between the  $s$ -meson and the nucleon, which is similar to that adopted in eq. (20) of ref. [14]. In general,  $F(s)$  is allowed to be an arbitrary function of the scalar field. However, in the present model we choose the simplest one, namely,  $F(s) = s$ . Note that, as demonstrated in the QMC model [15–17], this complexity is associated with the fact that the nucleon has the internal structure which responds to the mean scalar fields. In principle one could also multiply this interaction by an arbitrary function of  $\sigma^2 + \boldsymbol{\pi}^2$ . However, since the  $\sigma$  field is relatively suppressed because of its large mass, we ignore such possibilities in this initial investigation. We simply add this Lagrangian density with  $F(s) = s$  to the L $\sigma$ M.

It is also vital to add the repulsive NN interaction due to the  $\omega$ -meson exchange. It can be introduced as a gauge-like boson [5], that is, we add the kinetic energy term for the  $\omega$ -meson and replace the derivative by a covariant form:  $\partial_\mu \rightarrow D_\mu = \partial_\mu + ig_v\omega_\mu$ , with  $g_v$  the  $\omega$ -N coupling constant.

As usual, we shift the  $\sigma$  field ( $\sigma \rightarrow f_\pi - \sigma$ ) and eliminate  $\lambda$ ,  $v$  and  $c$  in favor of the free masses of the nucleon,  $\sigma$  and  $\pi$  mesons ( $M$ ,  $m_\sigma$  and  $m_\pi$ , respectively). (Notice that hereafter  $\sigma$  denotes the shifted, positive mean value.) The free masses are generated by spontaneous symmetry breaking. Taking MFA, the total Lagrangian density then reads

$$\begin{aligned} \mathcal{L} = & \bar{\psi}[i\gamma^\mu\partial_\mu - M^*(\sigma, s) - g_v\gamma_0\omega]\psi \\ & - \frac{1}{2}((\nabla\sigma)^2 + (\nabla s)^2) - \frac{1}{2}(m_\sigma^2\sigma^2 + m_s^2s^2) \\ & + \frac{1}{2}(\nabla\omega)^2 + \frac{1}{2}m_\omega^{*2}(\sigma, s)\omega^2 - V(\sigma), \quad (4) \end{aligned}$$

where the pion field vanishes, because the nuclear ground state has good parity. The time component of the  $\omega$  field is simply denoted by  $\omega$  and the “Mexican hat” potential,  $V$ , is

$$V(\sigma) = \frac{1-R}{8}\left(\frac{m_\sigma}{f_\pi}\right)^2\sigma^3(\sigma - 4f_\pi), \quad (5)$$

with  $R = (m_\pi/m_\sigma)^2$  and  $m_\pi = 138$  MeV. In the chiral limit,  $R$  becomes 0.

The effective nucleon and  $\omega$ -meson masses are respectively given by

$$\begin{aligned} M^*(\sigma, s) = & (M - g_s s)\left(1 - \frac{\sigma}{f_\pi}\right) \\ = & M - g_0\sigma - g_s s + \frac{1}{M}(g_0\sigma)(g_s s), \quad (6) \end{aligned}$$

$$m_\omega^{*2}(\sigma, s) = m_\omega^2\left[\left(1 - \frac{\sigma}{f_\pi}\right)^2 + \left(\frac{s}{f_\pi}\right)^2\right]. \quad (7)$$

**Table 1.** Properties of symmetric nuclear matter at normal nuclear matter density ( $\rho_0 = 0.17 \text{ fm}^{-3}$ ). The  $\sigma$  mass varies in the range of 0.9 and 1.15 GeV. Note that, in the present model,  $g_0^2 = 101.9$  and  $g_v^2 = 70.89$ , which together with the pion decay constant ( $f_\pi = 93 \text{ MeV}$ ) give the free nucleon and  $\omega$ -meson masses. We take  $m_\pi = 138 \text{ MeV}$ . All masses, energies and incompressibility are quoted in MeV.

$m_\sigma$	$m_s$	$g_s^2$	$\zeta$	$g_0\sigma$	$g_s s$	$V(\sigma)/\rho_0$	$M^*/M$	$K$
900	346.5	12.28	0.7	130	130	-6.69	0.743	214
950	388.0	17.29	0.75	111	143	-4.72	0.747	216
1000	441.7	24.48	0.8	96.4	155	-3.42	0.750	214
1050	510.7	35.00	0.85	84.4	164	-2.55	0.751	214
1100	612.1	53.08	0.85	74.6	172	-1.93	0.752	212
1150	741.9	81.35	0.85	66.5	179	-1.50	0.752	218

Here the free masses and the pion decay constant in vacuum are taken to be  $M = 939 \text{ MeV}$ ,  $m_\omega = 783 \text{ MeV}$  and  $f_\pi = 93 \text{ MeV}$ .

Because the pion decay constant is fixed, the coupling constants  $g_0$  and  $g_v$  are automatically determined through the relations  $M = f_\pi g_0$  and  $m_\omega = g_v f_\pi$ . The former is the Goldberger-Treiman (GT) relation in vacuum, where the axial-vector coupling constant  $g_A$  is unity. Note that if a chiral-invariant interaction with an additional parameter  $\xi$  is introduced [11,18],

$$\Delta\mathcal{L} = i\xi\bar{\psi}\gamma^\mu[W\partial_\mu W^\dagger P^L + W^\dagger\partial_\mu W P^R]\psi, \quad (8)$$

where  $W = \sigma + i\boldsymbol{\tau} \cdot \boldsymbol{\pi}$  and  $P^{R/L} = (1 \pm \gamma_5)/2$ , one can generate  $g_A$  different from unity in the tree approximation. In the present model, the axial-vector current  $A_a^\mu$  is given by the usual form. The contributions from the nucleon and pion fields are then expressed by  $A_a^\mu = \bar{\psi}\gamma^\mu\gamma_5(\tau_a/2)\psi + (f_\pi - \sigma)\partial^\mu\pi_a$ . Taking the divergence of this current and using the Dirac equation for the nucleon, one obtains the equation for the  $\pi$  field, from which we can find the GT relation in matter,

$$g_{\pi N}^* = \frac{g_A M^*}{f_\pi - \sigma} = g_0 \left(1 - g_s \frac{s}{M}\right), \quad (9)$$

where  $g_{\pi N}^*$  is the  $\pi$ -nucleon coupling constant in matter. Unless the chiral-singlet scalar meson is introduced,  $g_{\pi N}^* = g_0$  even in matter. Once the  $s$  field is involved, the coupling  $g_{\pi N}^*$  decreases depending on it.

The Lagrangian density eq. (4) gives the total energy per nucleon (for symmetric nuclear matter) at baryon density  $\rho_B$ :

$$\frac{E}{A} = \frac{4}{(2\pi)^3 \rho_B} \int d\mathbf{k} \sqrt{M^{*2} + \mathbf{k}^2} + \frac{1}{2\rho_B} (m_\sigma^2 \sigma^2 + m_s^2 s^2) + \frac{g_v^2 \rho_B}{2m_\omega^2} + \frac{V(\sigma)}{\rho_B}. \quad (10)$$

There are three parameters to be determined: the scalar meson masses,  $m_\sigma$  and  $m_s$ , and the coupling constant  $g_s$ . First, let us try to fix  $m_\sigma$  to be a relatively large mass around 1 GeV. The remaining parameters,  $m_s$  and  $g_s$ , are then chosen so as to produce the saturation property of symmetric nuclear matter:  $E/A - M = -15.7 \text{ MeV}$  at  $\rho_0 = 0.17 \text{ fm}^{-3}$  ( $\rho_0$  the normal nuclear matter density).

This Lagrangian, however, produces a very small incompressibility, around 100 MeV. As seen in eq. (7), the coupling of the  $\sigma$ -meson to the  $\omega$  reduces the  $\omega$  mass in matter, while the light scalar meson enhances it. Since the  $\omega$  mass is eventually not reduced much at large  $\rho_B$ , the repulsive force is insufficient and the model cannot produce the correct incompressibility ( $K = 210 \pm 30 \text{ MeV}$ ). If the effective  $\omega$  mass is reduced significantly, the EOS becomes stiff [19]. Since the  $\omega$ -meson has internal structure, it is not surprising that the mass generally involves higher-order dependence on the scalar fields [16,17]. If we add a (chiral-invariant) next-order term

$$\mathcal{L}_{next} = -\frac{\zeta}{2f_\pi} g_v^2 \omega^2 s^3 \quad (11)$$

to the Lagrangian density, this changes the effective  $\omega$ -meson mass as

$$m_\omega^{*2} = m_\omega^2 \left[ \left(1 - \frac{\sigma}{f_\pi}\right)^2 + \left(1 - \zeta \frac{s}{f_\pi}\right) \left(\frac{s}{f_\pi}\right)^2 \right]. \quad (12)$$

The new parameter  $\zeta$  can control  $m_\omega^*$  around  $\rho_0$  and provide a more realistic incompressibility.

### 3 Numerical results

Now we are in a position to show our results for nuclear matter. Varying the  $\sigma$ -meson mass, we determine the three parameters,  $m_s$ ,  $g_s$  and  $\zeta$ , so as to reproduce the saturation condition and the correct  $K$ . In table 1, we show the nuclear matter properties at  $\rho_0$ . We also present the scalar and vector mean fields as functions of nuclear matter density in fig. 1. In our calculation, the  $\sigma$  mass varies around 1 GeV. As discussed above, the mass of the light scalar meson should be about 400–500 MeV to get good fits to properties of finite nuclei. From the table, in the case of  $m_\sigma = 1.0$ –1.05 GeV, the  $s$ -meson mass is in the desired range. This is not a trivial fact. In contrast, in the case where  $m_\sigma \geq 1.1 \text{ GeV}$  ( $m_\sigma \leq 0.95 \text{ GeV}$ ),  $m_s$  seems too large (small). Furthermore, as expected, with increasing  $\sigma$  mass, the contribution of the  $\sigma$  field to the total energy is suppressed (see table 1 and fig. 1) and the ‘‘Mexican hat’’ potential is correspondingly much reduced. Note that, in the chiral model of Boguta [5], we find  $g_0\sigma \simeq 200 \text{ MeV}$  and  $V/\rho_B \simeq -21 \text{ MeV}$  at  $\rho_0$ .

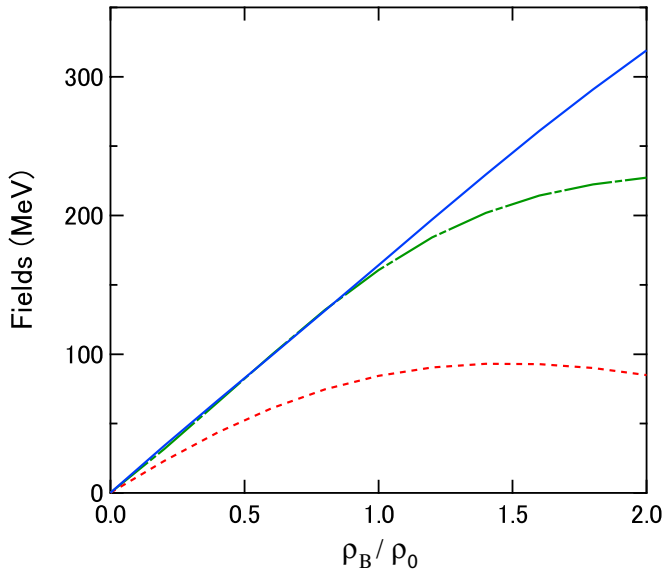


**Fig. 1.** Scalar and vector mean fields. The dashed and solid curves are, respectively, for the  $\sigma$  ( $g_0\sigma$ ) and  $s$  ( $g_s s$ ) fields, while the dot-dashed one is for the  $\omega$  ( $g_\omega\omega$ ) field. The  $\sigma$  mass is taken to be 1050 MeV (see table 1).

The nucleon mass is reduced by about 25% at  $\rho_0$ . In eq. (6), the linear terms of the scalar fields reduce the mass while the quadratic term increases it. It should be emphasized here that the reduction of the nucleon mass depends on the  $s$  field as well as the  $\sigma$ , where the  $\sigma$  may be directly related to the change of the quark condensate in matter (see discussions below), while the  $s$ -meson contribution is related to the mid-range NN attractive force. In this model, the two different origins of the mass reduction are simultaneously present.

The contribution of the quadratic term in  $M^*$  has already been studied in detail in the QMC model from the point of view of the quark substructure of the nucleon [15–17]. In the QMC model, the effective nucleon mass is approximated as  $M^* \approx M - g_s s + \frac{a}{2}(g_s s)^2$ , where the coefficient of the quadratic term,  $a/2$ , is known as the scalar polarizability [15, 20] ( $a$  is estimated to be  $10^{-3} \text{ MeV}^{-1}$  [16]). In the present case, since numerically  $g_0\sigma \simeq 0.5 \times g_s s$  for the proper  $\sigma$  mass (see table 1), the scalar polarizability is of order  $1/2M \simeq 0.5 \times 10^{-3} \text{ MeV}^{-1}$ , which is just the same as that in the QMC model.

We now wish to relate the change of the nucleon mass to the evolution of the quark condensate  $\langle \bar{q}q(\rho_B) \rangle$  in matter. The quark condensate and its evolution at finite density can be obtained by identifying the symmetry breaking pieces of QCD with that of our Lagrangian:  $-2m_q \bar{q}q = c\sigma = f_\pi m_\pi^2 \sigma$ . This shows that the condensate evolution is driven by the mean value of  $\sigma$ , the chiral partner of the pion. From this relation and the Gell-Mann–Oakes–Renner relation, we get the relative modification of the condensate (to the vacuum value) at finite density:

$$\frac{\langle \bar{q}q(\rho_B) \rangle}{\langle \bar{q}q(0) \rangle} = 1 - \frac{\sigma}{f_\pi}. \quad (13)$$

Since both the  $\sigma$  and  $s$  fields at low density are exclusively governed by the scalar density of the nucleon field  $\langle \bar{\psi}\psi \rangle$

$$\sigma \simeq \frac{g_0}{m_\sigma^2} \langle \bar{\psi}\psi \rangle \quad \text{and} \quad s \simeq \frac{g_s}{m_s^2} \langle \bar{\psi}\psi \rangle, \quad (14)$$

the  $s$  field at low density can be related to the  $\sigma$  field

$$s \simeq \left( \frac{g_s}{g_0} \right) \left( \frac{m_\sigma}{m_s} \right)^2 \sigma. \quad (15)$$

Using eqs. (6), (13) and (15), we can *numerically* relate the nucleon mass at low density to the condensate evolution,

$$\frac{M^*}{M} \simeq \frac{\langle \bar{q}q(\rho_B) \rangle}{\langle \bar{q}q(0) \rangle} \left[ 1 - \left( \frac{g_s m_\sigma}{g_0 m_s} \right)^2 \left( 1 - \frac{\langle \bar{q}q(\rho_B) \rangle}{\langle \bar{q}q(0) \rangle} \right) \right]. \quad (16)$$

This rather complicated structure comes from the fact that the mass reduction depends on two different sources, both the quark condensate and the NN attractive force.

Next let us see some properties of finite nuclei. The variation of the Lagrangian results in the following equations for static, spherically symmetric nuclei in MFA:

$$[-i\boldsymbol{\alpha} \cdot \boldsymbol{\nabla} + \gamma_0 M^*(\mathbf{r}) + g_v \omega(\mathbf{r}) + \frac{1}{2}e(1 + \tau_3)A_0(\mathbf{r})]U_\alpha(\mathbf{r}) = E_\alpha U_\alpha(\mathbf{r}), \quad (17)$$

$$(\nabla^2 - m_\sigma^2)\sigma(\mathbf{r}) = \left( \frac{\partial M^*}{\partial \sigma} \right) \rho_s(\mathbf{r}) - m_v^* \left( \frac{\partial m_v^*}{\partial \sigma} \right) \omega(\mathbf{r})^2 + \left( \frac{\partial V}{\partial \sigma} \right), \quad (18)$$

$$(\nabla^2 - m_s^2)s(\mathbf{r}) = \left( \frac{\partial M^*}{\partial s} \right) \rho_s(\mathbf{r}) - m_v^* \left( \frac{\partial m_v^*}{\partial s} \right) \omega(\mathbf{r})^2, \quad (19)$$

$$(\nabla^2 - m_v^{*2})\omega(\mathbf{r}) = -g_v \rho_B(\mathbf{r}), \quad (20)$$

$$\nabla^2 A_0(\mathbf{r}) = -e\rho_p(\mathbf{r}), \quad (21)$$

where we include the Coulomb field  $A_0$ . The solution to the Dirac equation is denoted by  $U_\alpha$ , whose state and energy are, respectively, specified by a set of quantum numbers  $\alpha$  and  $E_\alpha$ . The scalar, baryon and proton densities are respectively given by

$$\rho_s(\mathbf{r}) = \sum_{\alpha}^{occ.} \bar{U}_\alpha(\mathbf{r})U_\alpha(\mathbf{r}), \quad (22)$$

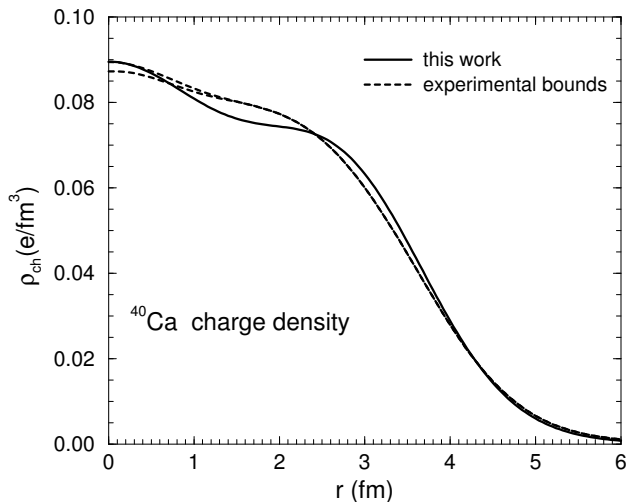
$$\rho_B(\mathbf{r}) = \sum_{\alpha}^{occ.} U_\alpha(\mathbf{r})^\dagger U_\alpha(\mathbf{r}), \quad (23)$$

$$\rho_p(\mathbf{r}) = \sum_{\alpha}^{protons} U_\alpha(\mathbf{r})^\dagger U_\alpha(\mathbf{r}). \quad (24)$$

As an illustrative example we consider the case of  $^{40}\text{Ca}$ . Firstly, instead of  $\rho_0 = 0.17 \text{ fm}^{-3}$ , we adopt the value of  $\rho_0 = 0.155 \text{ fm}^{-3}$ , which is closer to the interior density of  $^{208}\text{Pb}$ , and again search the parameter set for nuclear

**Table 2.** Single-particle energies for  $^{40}\text{Ca}$ . All energies are quoted in MeV.

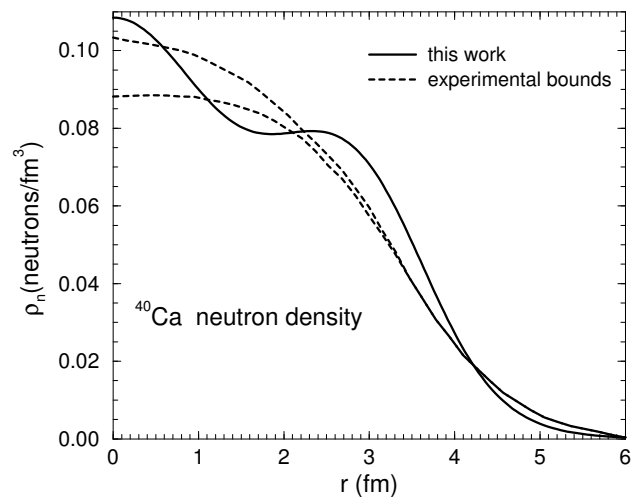
	$1s_{1/2}$	$1p_{3/2}$	$1p_{1/2}$	$1d_{5/2}$	$1d_{3/2}$	$2s_{1/2}$
Proton	-35.8	-24.8	-23.2	-12.7	-10.0	-7.7
Neutron	-44.8	-33.2	-31.7	-20.5	-17.9	-15.8

**Fig. 2.** Charge density distribution for  $^{40}\text{Ca}$ . The experimental data are denoted by the area delimited by the dashed lines [21].

matter. We then find:  $m_\sigma = 0.92$  GeV,  $m_s = 404.0$  MeV,  $g_s^2 = 18.07$  and  $\zeta = 0.7$ , which reproduces the saturation condition with  $K = 218$  MeV. We next solve a set of coupled nonlinear differential equations for a finite nucleus, that is derived from the total Lagrangian density (see eqs. (17)-(24)). It may be solved by a standard iteration procedure [15–17]. This leads to a value for the binding energy per nucleon of  $E_B/A = -8.28$  MeV (the observed value is  $-8.45$  MeV).

In table 2, the calculated spectra are summarized. Because of the relatively smaller scalar and vector fields in the present model than in Quantum Hadrodynamics (QHD) [1], the spin-orbit splittings are smaller. The good agreement in the binding energy per nucleon comes at the expense of a reduction in the spin-orbit force. Note that there is a strong correlation between the effective nucleon mass and the spin-orbit force. It is expected that the inclusion of the exchange contributions (Fock terms) will increase the absolute values of the single-particle, scalar and vector potentials [22]. This increase, together with the contribution to the spin-orbit force from the Fock term itself, may be expected to improve the spin-orbit splitting in finite nuclei. We leave this for a future study.

The charge density distribution is illustrated in fig. 2. Having solved the coupled differential equations, we obtain the point-proton and neutron densities in a nucleus. It is then necessary to consider the effect of the nucleon form factor that gives a considerable correction to the density distribution. We calculate the charge density by a convolution of the point-proton and neutron densities with the

**Fig. 3.** Point-neutron density distribution in  $^{40}\text{Ca}$ . The area delimited by the dashed lines represents the empirical fit to proton scattering data performed in ref. [23].

proton and neutron charge distributions [15,24]. We then obtain the root-mean-square (r.m.s.) charge radius ( $r_{ch} = 3.44$  fm) and the difference between nuclear r.m.s. radii for neutrons and protons ( $r_n - r_p = -0.157$  fm) —the observed values are, respectively, 3.48 fm and  $0.05 \pm 0.05$  fm.

As seen in fig. 2, the calculated charge density distribution is close to the experimental area. We note that there are no strong oscillations, even in the charge density of  $^{208}\text{Pb}$ . (In conventional nuclear models based on the  $L\sigma M$ , unrealistic oscillations in the charge density have been reported [10].) In fig. 3, we show the neutron density distribution. Again we find reasonable agreement with the experimental data. The results for the charge and neutron densities in our model are very similar to those of the other chiral models [12].

## 4 Discussions and conclusions

We have developed a chiral nuclear model based on the  $L\sigma M$ . In general, an effective field theory at low energy contains an infinite number of interaction terms, which incorporate the *compositeness* of hadrons [16,17]. It is then expected to involve numerous couplings which may be nonrenormalizable. To make sensible calculations, Manohar and Georgi [25] have proposed a systematic way to manage such complicated, effective field theories called “naive dimensional analysis” (NDA). NDA gives rules for assigning a coefficient of the appropriate size to any interaction term in an effective Lagrangian. After extracting the dimensional factors and some appropriate counting factors using NDA, the remaining *dimensionless* coefficients are all assumed to be of order *unity*. This is the so-called *naturalness* assumption. If naturalness is valid, the effective Lagrangian can be truncated at a given order with a reasonable bound on the truncation error for physical observables. Then we can control the effective Lagrangian, at least at the tree level.

**Table 3.** Interaction terms and corresponding (dimensionless) coupling constants for  $m_\sigma = 1050$  MeV (see table 1).

Term	$c_{\ell mnp}$	Value
$\bar{\psi}\sigma\psi$	$c_{1100}$	0.94
$\bar{\psi}s\psi$	$c_{1001}$	0.55
$\bar{\psi}\sigma s\psi$	$c_{1101}$	0.55
$\bar{\psi}\gamma_0\omega\psi$	$c_{1010}$	0.78
$\sigma\omega^2$	$c_{0120}$	1.2
$\sigma^2\omega^2$	$c_{0220}$	1.2
$s^2\omega^2$	$c_{0022}$	1.2
$s^3\omega^2$	$c_{0023}$	3.1
$\sigma^3$	$c_{0300}$	3.3
$\sigma^4$	$c_{0400}$	3.3

Here we use NDA to see whether this model gives natural coefficients. When a generic, interaction Lagrangian density is written as [26]

$$\mathcal{L}_{int.} \sim \frac{c_{\ell mnp}(f_\pi\Lambda)^2}{m!n!p!} \left( \frac{\bar{\psi}\Gamma\frac{\tau}{2}\psi}{f_\pi^2\Lambda} \right)^\ell \left( \frac{\sigma}{f_\pi} \right)^m \left( \frac{\omega}{f_\pi} \right)^n \left( \frac{s}{f_\pi} \right)^p, \quad (25)$$

the overall coupling constant  $c_{\ell mnp}$  is dimensionless and of  $\mathcal{O}(1)$  if naturalness holds. Here  $\Gamma$  and  $\tau$ , respectively, stand for a combination of Dirac matrices and isospin operators, and  $\Lambda$  ( $\sim 1$  GeV) is a large mass scale for the strong interaction.

The present model has 10 interaction terms and the result is shown in table 3. Only three coefficients,  $c_{0023}$ ,  $c_{0300}$  and  $c_{0400}$ , are close to 3:  $c_{0023}$  comes from eq. (11) while the latter two are for the ‘‘Mexican hat’’ potential. They all are, however, of order unity and almost natural. This model is thus *natural* as an effective field theory for nuclei.

To describe the properties of nuclear matter and finite nuclei at mean-field level, it seems to be necessary to introduce two different scales associated with the scalar mesons: one is the usual  $\sigma$ -meson that is the chiral partner of the pion, and the other is a new one that is treated as a chiral singlet and is responsible for the mid-range NN attraction. The present model has three parameters, which are determined so as to produce the saturation condition at normal nuclear matter density and the proper incompressibility. Then, the model automatically predicts two scalar scales, that is, one concerns the chiral symmetry ( $m_\sigma \sim 1$  GeV) and the other relates to the NN attraction ( $m_s \sim 400$ – $500$  MeV). Because the  $\sigma$  mass is heavy, the contribution of the  $\sigma$  field to the total energy is relatively suppressed and the ‘‘Mexican hat’’ potential is very much reduced as well. This fact is vital to obtain better fits to the properties of finite nuclei. We have demonstrated the single-particle spectra, charge and neutron densities of  $^{40}\text{Ca}$  as well as the properties of symmetric nuclear matter. The present approach improves conventional nuclear models based on the  $L\sigma M$ .

As a next step, it would be necessary to extend this approach to include the  $\rho$ -meson in order to study unstable nuclei and/or dense matter like neutron stars. The simplest way is to couple it to the (isovector) conserved

current. However, it may be more elegant to include the coupling in a (local) gauge-invariant manner [9].

It should be noted that in this model the reduction of the hadron mass depends on the  $s$  field as well as on the  $\sigma$ , where the  $\sigma$  is related to the change of the quark condensate in matter and the  $s$ -meson contribution is related to the mid-range NN attractive force. The two different origins contribute to the mass reduction simultaneously. It would be of great interest to study, from the point of view of the quark substructure of hadrons, the relation between the dependence of hadron masses on the scalar fields in this chiral model and that in the QMC model [15–17]. Furthermore, if the effective  $\omega$  mass is sufficiently reduced around normal nuclear matter density [27], it would be possible to form an  $\omega$ -nucleus bound state [28] and such exotic states may provide significant information on chiral symmetry restoration (see eqs. (12) and (13)). Finally, we observe that the  $\sigma$  mass *predicted* in this model is very close to the scalar glueball mass assumed in ref. [12] (although it was integrated out and does not appear explicitly). Therefore, it would also be very intriguing to study whether there is a deeper connection between the  $\sigma$  and such scalar glueball.

This work was supported by the DOE contract DE-AC05-84ER40150, under which SURA operates the Jefferson Laboratory, and Academic Frontier Project (Holcs, Tokyo University of Science, 2005) of MEXT.

## References

1. B.D. Serot, J.D. Walecka, *Advances in Nuclear Physics*, Vol. **16** (Plenum, N.Y., 1985) p. 1.
2. See, for example, C. Fuchs, H. Lenske, H.H. Wolter, *Phys. Rev. C* **52**, 3043 (1995); B.D. Serot, J.D. Walecka, *Int. J. Mod. Phys. E* **6**, 515 (1997).
3. T.D. Lee, G.C. Wick, *Phys. Rev. D* **9**, 2291 (1974); T.D. Lee, M. Margulies, *Phys. Rev. D* **11**, 1591 (1975).
4. A.K. Kerman, L.D. Miller, MIT-CTP Pub. Report No. 449 (1974), unpublished.
5. J. Boguta, *Phys. Lett. B* **120**, 34 (1983).
6. S. Sarkar, S.K. Chowdhury, *Phys. Lett. B* **153**, 358 (1985).
7. T. Matsui, B.D. Serot, *Ann. Phys. (N.Y.)* **144**, 107 (1982).
8. V.N. Fomenko, S. Marcos, L.N. Savushkin, *J. Phys. G* **19**, 545 (1993); V.N. Fomenko, L.N. Savushkin, S. Marcos, R. Niembro, M.L. Quelle, *J. Phys. G* **21**, 53 (1995); L.N. Savushkin, H. Toki, *The Atomic Nucleus as a Relativistic System* (Springer, Berlin, 2004).
9. P. Bernardos, V.N. Fomenko, M.L. Quelle, S. Marcos, R. Niembro, L.N. Savushkin, *J. Phys. G* **22**, 361 (1996); V.N. Fomenko, P. Ring, L.N. Savushkin, *Nucl. Phys. A* **579**, 438 (1994); V.N. Fomenko, S. Marcos, P. Ring, L.N. Savushkin, *Phys. At. Nucl. (Engl. Transl.)* **60**, 2149 (1997).
10. R.J. Furnstahl, B.D. Serot, H.B. Tang, *Nucl. Phys. A* **598**, 539 (1996); see also E.K. Heide, S. Rudaz, P.J. Ellis, *Nucl. Phys. A* **571**, 713 (1994).
11. G. Chanfray, M. Ericson, P.A.M. Guichon, *Phys. Rev. C* **63**, 055202 (2001).
12. R.J. Furnstahl, H.B. Tang, B.D. Serot, *Phys. Rev. C* **52**, 1368 (1995); P. Papazoglou, D. Zschesche, S. Schramm, J. Schaffner-Bielich, H. Stöcker, W. Greiner, *Phys. Rev. C* **59**, 411 (1999).

13. G. Chanfray, M. Ericson, nucl-th/0402018.
14. J. Delorme, M. Ericson, P.A.M. Guichon, A.W. Thomas, Phys. Rev. C **61**, 025202 (2000).
15. P.A.M. Guichon, K. Saito, E. Rodionov, A.W. Thomas, Nucl. Phys. A **601**, 349 (1996); K. Saito, K. Tsushima, A.W. Thomas, Nucl. Phys. A **609**, 339 (1996).
16. K. Saito, K. Tsushima, A.W. Thomas, Phys. Rev. C **55**, 2637 (1997).
17. For a review, K. Saito, K. Tsushima, A.W. Thomas, to be published in Prog. Part. Nucl. Phys., hep-ph/0506314.
18. K. Tsushima, D.O. Riska, Phys. Lett. B **333**, 17 (1994).
19. See, for example, H. Kouno, Y. Horinouchi, K. Tsuchitani, Prog. Theor. Phys. **112**, 831 (2004).
20. A.W. Thomas, P.A.M. Guichon, D.B. Leinweber, R.D. Young, nucl-th/0411014.
21. I. Sick *et al.*, Phys. Lett. B **88**, 245 (1979).
22. G. Krein, A.W. Thomas, K. Tsushima, Nucl. Phys. A **650**, 313 (1999).
23. L. Ray, P.E. Hodgson, Phys. Rev. C **20**, 2403 (1979).
24. S. Platchkov *et al.*, Nucl. Phys. A **508**, 343c (1990).
25. A. Manohar, H. Georgi, Nucl. Phys. B **234**, 189 (1984); H. Georgi, L. Randall, Nucl. Phys. B **276**, 241 (1986); H. Georgi, Phys. Lett. B **298**, 187 (1993).
26. K. Saito, K. Tsushima, A.W. Thomas, Phys. Lett. B **406**, 287 (1997).
27. D. Trnka *et al.*, Phys. Rev. Lett. **94**, 192303 (2005).
28. K. Tsushima, D.H. Lu, A.W. Thomas, K. Saito, Phys. Lett. B **443**, 26 (1998); K. Saito, K. Tsushima, D.H. Lu, A.W. Thomas, Phys. Rev. C **59**, 1203 (1999); F. Klingl, T. Waas, W. Weise, Nucl. Phys. A **650**, 299 (1999); R.S. Hayano, S. Hirenzaki, A. Gillitzer, Eur. Phys. J. A **6**, 99 (1999).